



Application of chelating ion-exchangers Amberlite IRC-718 and Duolite ES-346 in removal of Pt(IV) ions from chloride and chloride-nitrate media

Zbigniew Hubicki^{a,b}, Monika Wawrzekiewicz^{a,*}, Bożena Łodyga^b, Andrzej Łodyga^b

^aFaculty of Chemistry, Department of Inorganic Chemistry, Maria Curie-Skłodowska University,
Maria Curie-Skłodowska Sq. 2, 20-031 Lublin, Poland

Tel. +48 81 537 57 38; Fax: +48 81 533 33 48; email: m.wawrzekiewicz@op.pl

^bFertilizer Research Institute, 24-100 Pulawy, Poland

Received 13 September 2011; Accepted 7 December 2011

ABSTRACT

The chelating ion exchangers of the functional iminodiacetate (Amberlite IRC-718) and amidoxime (Duolite ES-346) groups have been applied for Pt(IV) removal from the chloride (0.1 ÷ 8.0 M HCl) and chloride-nitrate (0.1 M HCl + 0.9 M HNO₃, 0.5 M HCl + 0.5 M HNO₃, 0.9 M HCl + 0.1 M HNO₃) solutions. The monolayer sorption capacities (Q_0) for Amberlite IRC-718 determined from the Langmuir isotherm model were changed from 1.032 to 0.917 mmol g⁻¹ and from 0.948 to 0.831 mmol g⁻¹ in the chloride and chloride-nitrate solutions, respectively. For Duolite ES-346 Q_0 values were equal to 1.120–0.937 mmol g⁻¹ in the chloride solutions and 0.692–0.806 mmol g⁻¹ in the chloride-nitrate systems. The influence of acid concentrations, phase contact time and macrocomponent addition (AlCl₃, CuCl₂, NiCl₂) on Pt(IV) sorption was also studied. The pseudo second order equation provided the best fitting of experimental values. The working and total ion exchange capacities as well as distribution coefficients of Pt(IV) were determined by the dynamic method. From the breakthrough curves the time required for the formation and moving of the exchange zone was also calculated. Pt(IV) desorption in the amount of 84.3% and 77.6% from IRC-718 and ES-346, respectively, was performed using 6 M HCl.

Keywords: Chelating ion exchanger; Platinum; Precious metals; Recovery; Sorption; Kinetic studies

1. Introduction

Because of small amounts of platinum group metals (PGMs) in nature and their impoverishment in natural resources, physicochemical methods are of great importance for recovery of PGMs from secondary sources for example, used up three-way catalysts, dental alloys and industrial wastewaters [1,2]. One of these methods is ion exchange chromatography. Ion exchangers have long been used for the preconcentration and selective

sorption of platinum group metal ions from analytical and environmental samples [1–6]. Ion-exchange separations of palladium, platinum, rhodium and iridium ions were most frequently based on application of anion exchangers in chloride solutions making use of the change of valency value till a proper distribution coefficient is reached [1]. Recently very good results have been obtained in both sorption and separation of trace and milligram amounts of noble metal ions using chelating ion exchangers [6–10]. These resins are characterised by diversified affinity and high selectivity for platinum metals. Their properties depend on the type of

*Corresponding author.

functional groups, though to a lesser extent on grain size and physical properties. Slow sorption kinetics is their undesired characteristics [2,4]. According to Kononova et al. Bayer was the first who pointed out to the importance of this type of ion exchangers based on the investigation of stability and chemical composition of chelate complexes [2]. Mutual position of functional groups and their configuration affect sorption selectivity while the matrix properties are of smaller effect. The ion exchange capacity of these resins depends mainly on quantity of functional groups and pH of solution. The most widespread chelating functional groups are: thiol, thiourea, isothiurea, thiosemicarbazide, dithiocarbamide, dithi-zone and triisobutyl phosphine sulfide [1,2,11].

The aim of the present work is Pt(IV) ions removal from the chloride and chloride-nitrate solutions under the batch and column operations by means of the chelating resins Amberlite IRC-718 and Duolite ES-346. The influence of macrocomponent addition on Pt(IV) ions sorption in chloride solutions was also investigated. The choice of the systems used in our studies comes from the fact that solutions of similar chemical composition are frequently used in hydrometallurgical processes of PGMs recovery on a commercial scale for example, Mathhey Rustenberg Refiners [4,11,12].

2. Experimental

2.1. Materials

The aqueous Pt(IV) stock solution was prepared from H_2PtCl_6 (>99.9 %, POCh Poland) and standardized HCl solution in the amounts required for maintaining H^+ concentration at 0.1 M. Pt(IV) working solutions were obtained from the stock solution by dilution with

HCl or HCl and HNO_3 to adjust acid concentration to the desired value. The Pt(IV) working solutions with the macrocomponents: 1.0 M $AlCl_3$, 1.0 M $CuCl_2$ and 1.0 M $NiCl_2$ were prepared dissolving appropriate amounts of $AlCl_3$, $CuCl_2 \times 2H_2O$ or $NiCl_2 \times 6H_2O$ (POCh, Poland) in 0.1–1 M HCl. The other reagents produced by POCh (Poland) were of analytical grade.

Important physical and chemical properties of the chelating resins are presented in Table 1.

2.2. Adsorption studies

The batch sorption experiments were carried out in 0.1 l conical flasks where 0.5 g of the dry ion exchanger and 0.05 l of Pt(IV) solution ($1.09\text{--}73.66 \text{ mmol Pt(IV) l}^{-1}$ in 0.1–3 M HCl or 0.1–0.9 M HCl + 0.9–0.1 M HNO_3) were added without adjusting pH. The flasks were agitated in the thermostated shaker (Elphin 358 S, Poland) at a constant speed of 170 rpm at 20°C for 120 min to achieve equilibrium. The Pt(IV) concentration after equilibrium adsorption was measured using the AAS method. The amount of Pt(IV) adsorbed at equilibrium, q_e (mmol g^{-1}), was calculated from Eq. (1):

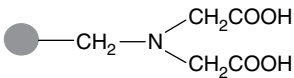
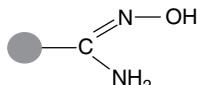
$$q_e = \frac{(C_0 - C_e)}{w} \times v \quad (1)$$

where C_0 and C_e are the concentrations of Pt(IV) at the beginning and in the equilibrium respectively (mmol l^{-1}); v is the volume of the solution (l); w is the mass of the dry ion exchanger (g).

2.2.1. Langmuir isotherm

The Langmuir isotherm is derived on the assumption of monolayer coverage of adsorbate over a homogenous

Table 1
Characteristics of ion exchangers

Ion exchanger	Amberlite IRC-718	Duolite ES-346
Producer	Rohm & Haas, France	Dia-Prosim, France
Functional groups	Iminodiacetate	Amidoxime
		
Matrix	Styrene–divinylbenzene	
Structure	Macroporous	
Harmonic mean size [mm]	0.3–1.2	
Total capacity [meq cm^{-3}]	1.0	1.11
Working range of pH	1.5–14	0–13
Max working temperature [°C]	90	40

● - polymer matrix.

adsorbent surface [13]. The linear form of the Langmuir isotherm equation is given as:

$$\frac{C_e}{q_e} = \frac{1}{Q_0 b} + \frac{1}{Q_0} C_e \quad (2)$$

where C_e is the equilibrium concentration of Pt(IV) (mmol l^{-1}); q_e is the amount of Pt(IV) adsorbed per unit mass of the ion exchanger at equilibrium (mmol g^{-1}); Q_0 (mmol g^{-1}) and b (l mmol^{-1}) are the Langmuir constants.

2.2.2. Freundlich isotherm

The Freundlich isotherm is expressed by the following equation:

$$q_e = K_F C_e^{1/n} \quad (3)$$

Eq. (3) can be linearized as Eq. (4):

$$\log q_e = \log K_F + \left(\frac{1}{n}\right) \log C_e \quad (4)$$

where C_e is the equilibrium concentration of Pt(IV) (mmol l^{-1}); q_e is the amount of Pt(IV) adsorbed per unit mass of the ion exchanger (mmol g^{-1}); K_F (mmol g^{-1}) and n are the Freundlich constants [13,14].

2.2.3. Temkin–Pyzhev isotherm

Heat of adsorption and the adsorbent-adsorbate interactions were studied by Temkin and Pyzhev. They suggested that due to these interactions the heat of adsorption of all molecules in the layer decreased linearly with the coverage [14]. The Temkin isotherm equation is given as:

$$q_e = \left(\frac{RT}{b_T}\right) \ln A + \left(\frac{RT}{b_T}\right) C_e \quad (5)$$

where b_T is the Temkin constant related to heat of sorption (J mol^{-1}); A is the Temkin isotherm constant (l g^{-1}); R is the gas constant ($8.31 \text{ J (mol K)}^{-1}$); T (K) is the temperature.

2.3. Kinetic batch studies

For the kinetic studies, 50 ml of Pt(IV) solutions was introduced into a 100 ml joint-stopper conical flask containing 0.5 g of the dried ion exchanger. The flask was capped and agitated at a constant temperature of 25°C in the shaker at 170 cpm for 1–360 min. After that time, the solution samples were taken and the concentrations of the residual ions were determined. The amount of Pt(IV) adsorbed at time t , q_t (mmol g^{-1}) was calculated from Eq. (6):

$$q_t = \frac{(C_0 - C_t)}{w} \times v \quad (6)$$

where C_0 and C_t are the concentrations of Pt(IV) in the solution at the beginning and after time t , respectively (mmol l^{-1}); v is the volume of the solution (l); w is the mass of the dry ion exchanger (g).

The fitting of Pt(IV) sorption on the chelating ion exchangers was investigated by three common kinetic models, namely, the Lagergren pseudo-first order equation (Eq. (7)), Ho linear pseudo-second order equation (Eq. (8)) as well as Weber and Morris intraparticle diffusion model (Eq. (9)) [15–18]:

$$\log(q_e - q_t) = \log(q_e) - \frac{k_1}{2.303} t \quad (7)$$

$$\frac{t}{q_t} = \frac{1}{k_2 q_e^2} + \frac{1}{q_e} t \quad (8)$$

$$q_t = k_i t^{0.5} \quad (9)$$

where q_e and q_t are the amounts (mmol g^{-1}) of Pt(IV) adsorbed at equilibrium and at time t (min) respectively; k_1 is the constant rate of pseudo-first order adsorption (l min^{-1}); k_2 is the constant rate of the pseudo-second order adsorption (g (mmol min)^{-1}); k_i is the intraparticle diffusion rate ($\text{mmol g}^{-1} \text{ min}^{0.5}$).

The effects of hydrochloric (0.1–8 M) and nitric (0.1–0.9 M) acids concentrations as well as the macrocomponent addition (1.0 M AlCl_3 , 1.0 M CuCl_2 or 1.0 M NiCl_2) on the amount of Pt(IV) adsorbed at time t , q_t (mol g^{-1}) was investigated, too.

2.4. Column experiments

2.4.1. Sorption studies

The dynamic procedures were applied [1]. The 1-cm diameter columns were filled with swollen ion exchangers in the amount of 0.01 l. Then the Pt(IV) solution of the initial concentration 0.55 mmol l^{-1} in the chloride or chloride-nitrate medium was passed through the ion exchanger bed at the flow rate of $0.4 \text{ cm}^3 \text{ min}^{-1}$. The eluate was collected in the fractions and Pt(IV) content was determined.

The weight (K_d) and bed (K'_d) distribution coefficients of Pt(IV) were calculated from the breakthrough curves according to Eqs. (10) and (11):

$$K_d = \frac{U - U_0 - V}{m_j} \quad (10)$$

$$K'_d = \frac{U - U_0 - V}{v_j} \quad (11)$$

where U is the effluent volume at $C = C_0/2$ (cm^3); U_0 is the dead volume in the column (liquid volume in the column between the bottom edge of the ion-exchanger bed and the outlet) (cm^3); V is the void (inter-particle) ion exchanger bed volume (which amounts to ca. 0.4 of the bed volume) (cm^3); m_i is the weight of ion exchanger in the column (g); and v_i is the swollen bed volume (cm^3) [1].

The working (C_w) and total (C_t) ion exchange capacities are expressed in mmol of Pt(IV) per 1 l of swollen ion exchanger. The amount of Pt(IV) loaded on the anion exchanger was calculated by mass balance.

During the loading process of ion exchange bed, at any time the ion exchange takes place in only a portion of bed called the exchange zone or interchangeably the mass transfer zone. The exchange zone moves down through the anion exchange bed. The direction of its movement and the acidic solutions (chloride or chloride-nitrate) flow are the same. Ahead of the exchange zone, the ion exchange bed is exhausted whereas underneath it is still fresh. When the exchange zone reaches the end of the anion exchange bed, platinum(IV) ions appear in the effluent. Based on the column parameters and breakthrough curves the time required for the formation (t_f) and moving of the exchange zone (t_m) was calculated, too [19]. The time required for formation (t_f) of the exchange zone can be calculated according to the following equation:

$$t_f = \frac{V_z}{U_r S} \quad (12)$$

where $V_z = V_t - V_{bp}$ is the difference between the total volume (V_t) of effluent and that collected to the break point (V_{bp}) (cm^3); U_r is the flow rate ($\text{cm}^3 \text{min}^{-1}$); S is the total column cross-section area (cm^2) [19].

The time required for moving (t_m) of the exchange zone was obtained from Eq. (13):

$$t_m = \frac{V_t}{U_r S} \quad (13)$$

2.4.2. Desorption studies

For the dynamic desorption studies, 0.01 l bed of Amberlite IRC-718 or Duolite ES-346 loaded with Pt(IV) was washed gently with distilled water to remove any unadsorbed Pt(IV). Then 6 M HCl (for sorption of Pt(IV) from chloride solutions) or 1 M HNO_3 (for sorption of Pt(IV) from chloride-nitrate solutions) were passed through the ion exchanger bed at the rate of $0.4 \text{ cm}^3 \text{min}^{-1}$. The eluate was collected in the fractions and the Pt(IV) content was determined. Then the amount of Pt(IV) desorbed from the ion exchanger bed was calculated by the mass balance.

3. Results and discussion

3.1. Equilibrium studies

The adsorption isotherm indicates how the adsorption molecules distribute between the liquid phase and the solid phase when the equilibrium state is reached. The analysis of the isotherm data by fitting them to different isotherm models is an important step to find the suitable model that can be used for the design purpose [20–22]. Fig. 1 shows the adsorption of Pt(IV) on the chelating ion exchangers at equilibrium. It exhibits steep increase at low concentrations, indicating high affinity for a solute. At high concentrations of Pt(IV), the adsorbed amounts increase slightly, showing horizontal plateaus.

Adsorption isotherm studies were carried out using the three models: Langmuir, Freundlich and Temkin–Pyzhev ones. The applicability of the isotherm equation was judged by the determination coefficients (r^2) values.

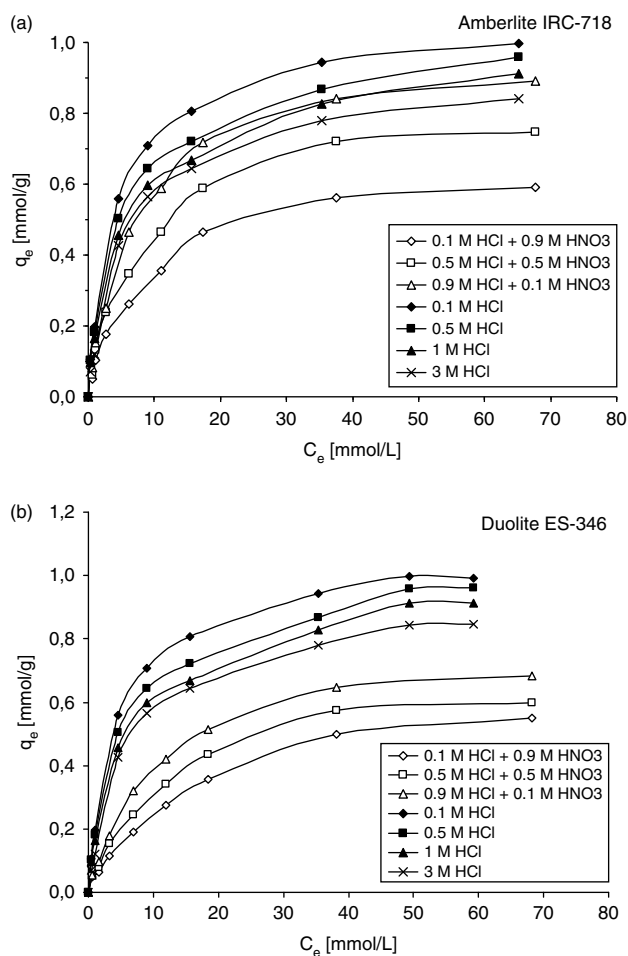


Fig. 1. Equilibrium uptake of Pt(IV) from the 0.1–3 M HCl and 0.1–0.9 M HCl – 0.9–0.1 M HNO_3 systems by Amberlite IRC-718 and Duolite ES-346.

The calculated constants, according to the Langmuir, Freundlich and Temkin–Pyzhev equations, are compared in Table 2. A straight line with the slope $1/Q_0$ was obtained from the plots C_e/q_e vs. C_e for Pt(IV) sorption on both chelating ion exchangers. The determination coefficient r^2 was equal to 0.990–0.999. It indicates that the adsorption data of Pt(IV) on Amberlite IRA-718 and Duolite ES-346 was well fitted to the Langmuir isotherm. The monolayer maximum adsorption capacities (Q_0) determined in the chloride and chloride-nitrate solutions corresponded with the experimental data.

For the Freundlich isotherm, the plots of $\log q_e$ vs. $\log C_e$ give a straight line with the n values listed in Table 2. It indicated that adsorption of Pt(IV) on the ion exchangers was also favourable. The values of r^2 were lower compared with the Langmuir model.

The constants A and b_T , listed in Table 2, according to the Temkin–Pyzhev equation were calculated from the plots of q_e vs. $\ln C_e$. The determination coefficient values were lower than 0.976 in the chloride and chloride nitrate systems. The heat of adsorption gives information about the adsorption mechanism as a chemical ion-exchange. If the value of b_T is between 8 and 16 kJ mol⁻¹ then the adsorption process follows by chemical ion-exchange and if $b_T < 8$ kJ mol⁻¹ the adsorption process is of physical nature [23]. The heat of adsorption b_T

determined from the Temkin–Pyzhev equation was in the range 8–16 kJ mol⁻¹ and revealed the nature of the ion exchange mechanism in this system. It is interesting to note that adsorption energy in some chloride-nitrate systems is higher than 16 kJ mol⁻¹ (Table 2). This deviation of the adsorption heat is satisfactory and close to the limits of the literature for ion exchange. A similar phenomenon was observed by Inglezakis [24].

3.2. Kinetic studies

3.2.1. Influence of acids concentration and phase contact time

Platinum like the other PGMs forms a range of complexes with a variety of different ligands. The Pt-chloro complexes such as $[\text{PtCl}_6]^{2-}$ for Pt(IV) and $[\text{PtCl}_4]^{2-}$ for Pt(II) are the most important, as aqueous chloride solution is the only cost-effective medium in which all PGMs can be brought into solution and concentrated [20]. Considering the 0.1 ÷ 3.0 M HCl – 0.55 mmol Pt(IV) l⁻¹ systems, the complex $[\text{PtCl}_6]^{2-}$ is predominant [6]. In the chloride-nitrate solutions (0.1 M HCl + 0.9 M HNO₃ – 0.55 mmol Pt(IV) l⁻¹, 0.5 M HCl + 0.5 M HNO₃ – 0.55 mmol Pt(IV) l⁻¹ and 0.9 M HCl + 0.1 M HNO₃ – 0.55 mmol Pt(IV) l⁻¹), containing Cl⁻ and NO₃⁻ ions,

Table 2

Comparison of the coefficients isotherm parameters for Pt(IV) sorption on Amberlite IRC-718 and Duolite ES-346 from the chloride and chloride-nitrate medium

System	Freundlich model			Langmuir model			Temkin–Pyzhev model		
	n	k_F [mmol g ⁻¹]	r^2	b [l mmol ⁻¹]	Q_0 [mmol g ⁻¹]	r^2	b_T [kJ mol ⁻¹]	A [l g ⁻¹]	r^2
Amberlite IRC-718									
0.1 M HCl	0.316	0.517	0.980	0.229	1.032	0.998	15.683	4.469	0.884
0.5 M HCl	0.335	0.425	0.982	0.145	1.000	0.996	15.735	2.883	0.892
1 M HCl	0.385	0.372	0.978	0.127	0.968	0.996	15.313	1.912	0.897
3 M HCl	0.542	0.363	0.933	0.146	0.917	0.999	13.607	1.023	0.917
0.1 M HCl + 0.9 M HNO ₃	0.537	0.155	0.950	0.119	0.948	0.997	19.128	0.896	0.970
0.5 M HCl + 0.5 M HNO ₃	0.518	0.226	0.935	0.118	0.662	0.997	15.952	1.210	0.976
0.9 M HCl + 0.1 M HNO ₃	0.472	0.374	0.948	0.183	0.831	0.990	13.912	1.566	0.970
Duolite ES-346									
0.1 M HCl	0.440	0.833	0.889	1.794	1.120	0.999	10.559	2.633	0.932
0.5 M HCl	0.557	0.604	0.892	0.877	0.912	0.998	11.859	1.311	0.908
1 M HCl	0.561	0.393	0.927	0.717	0.733	0.996	14.388	0.980	0.905
3 M HCl	0.553	0.337	0.947	0.125	0.937	0.998	13.079	0.997	0.910
0.1 M HCl + 0.9 M HNO ₃	0.583	0.083	0.983	0.058	0.692	0.997	20.644	0.570	0.930
0.5 M HCl + 0.5 M HNO ₃	0.572	0.133	0.967	0.070	0.753	0.995	18.065	0.685	0.960
0.9 M HCl + 0.1 M HNO ₃	0.574	0.199	0.949	0.100	0.806	0.999	16.043	0.815	0.973

chloro-platinum(IV), nitrate-platinum(IV), and chloride-nitrate platinum(IV) complexes appear but the chemical morphology of the chloride-nitrate platinum(IV) complexes is more complicated and not described in literature.

In the chloride and chloride-nitrate media the chelating ion exchangers Amberlite IRC-718 and Duolite ES-346 exhibited the properties of anion exchangers as explained in our previous studies [11], the protonation of nitrogen occurred in solutions of pH 2 or less. The mechanism of Pt(IV) ions sorption in the acidic medium on the above mentioned ion exchangers is anion-exchanging. Fig. 2 illustrates the amount of Pt(IV) adsorbed (q_t) by the chelating anion exchangers of the iminodiacetate and amidoxime groups as the function of phase contact time and hydrochloric acid concentration. In the 0.1 ÷ 8 M HCl – 0.55 mmol Pt(IV) l⁻¹ system, the values of q_t decreased with the increasing HCl content and changed from 0.0492 to 0.0113 mmol g⁻¹ and from 0.0488 to 0.0119 mmol g⁻¹ for Amberlite IRC-718 and Duolite ES-346, respectively. The decrease in sorption of [PtCl₆]²⁻ with higher HCl concentrations was due to the competitive sorption of Cl⁻ and HCl₂⁻ ions that was also reported by

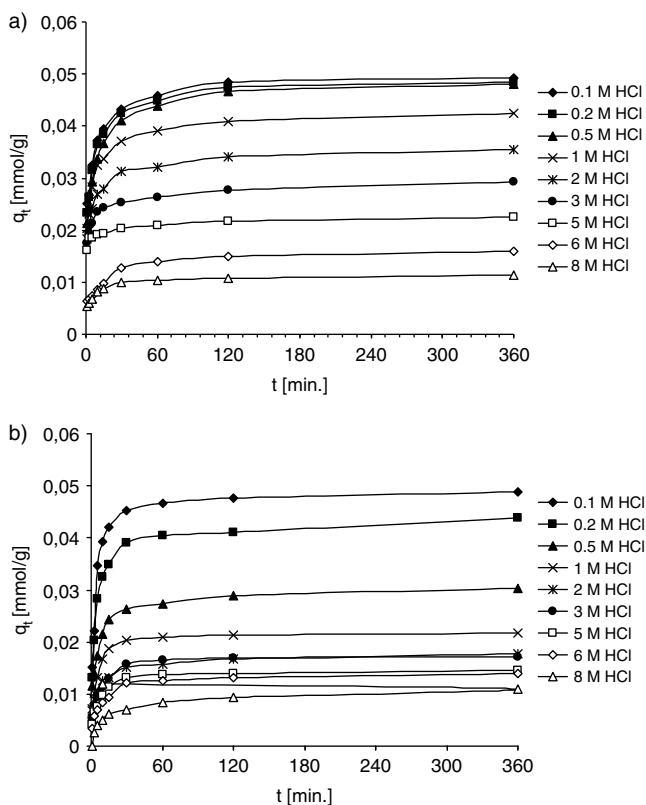


Fig. 2. Influence of phase contact time and HCl concentrations on the amount of Pt(IV) adsorbed from the 0.1–8 M HCl – 0.55 mmol Pt(IV) l⁻¹ systems using Amberlite IRC-718 (a) and Duolite ES-346 (b).

Minczewski et al. [1]. The values under discussion were relatively higher for the ion exchanger of iminodiacetate functional groups. The q_t increased with the increasing phase contact time and after 120 min equilibrium was reached.

In the mixed chloride–nitrate solutions (0.1 M HCl + 0.9 M HNO₃, 0.5 M HCl + 0.5 M HNO₃, and 0.9 M HCl + 0.1 M HNO₃) containing – 0.55 mmol Pt(IV) l⁻¹ the amount of Pt(IV) adsorbed by Amberlite RC-718 and Duolite ES-346 decreased with the increasing HNO₃ content for the same contact time being compared (Fig. 3). The influence of nitric acid on q_t values is particularly visible when Amberlite IRC-718 is used in sorption experiments. The sorption capacities using Amberlite IRC-718 varied from 0.0460 to 0.0276 mmol g⁻¹ with increasing of HNO₃ concentration. The equilibrium uptake in the case of both ion exchangers occurred after 120 min.

3.2.2. Influence of macrocomponent addition

The effect of macrocomponent addition was studied in the systems containing 0.55 mmol Pt(IV) l⁻¹ and 1 M of CuCl₂ or 1 M NiCl₂ or 1 M AlCl₃ by changing the quantity of hydrochloric acid (0.1 M, 0.2 M, 0.5 M, and 1 M) in the test solution as presented in Fig. 4. The addition of the macrocomponent to the chloride solution caused q_t values to decrease compared with the systems containing only hydrochloric acid. There was observed the q_t decrease with the HCl concentration increase from 0.1 to 1 M in the solutions 0.1–1.0 M HCl – 1 M NiCl₂ – 0.55 mmol Pt(IV) l⁻¹ and 0.1–1.0 M HCl – 1 M CuCl₂ – 0.55 mmol Pt(IV) l⁻¹ when Amberlite IRC-718 is used, there was observed the q_t increase with the HCl concentration increase from 0.1 to 1 M.

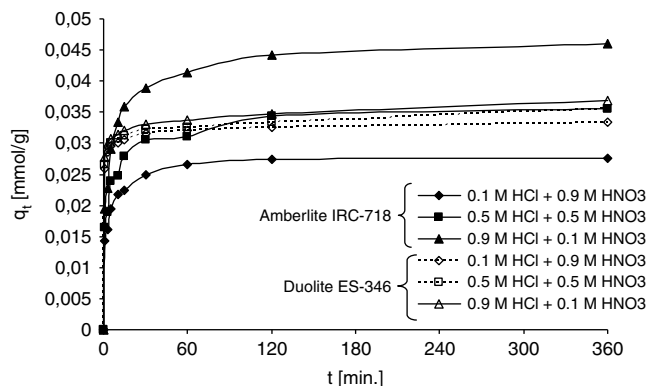


Fig. 3. Influence of phase contact time and HCl/HNO₃ concentrations on the amount of Pt(IV) adsorbed from the 0.1–0.9 M HCl – 0.9–0.1 M HNO₃ – 0.55 mmol Pt(IV) l⁻¹ systems using Amberlite IRC-718 and Duolite ES-346.

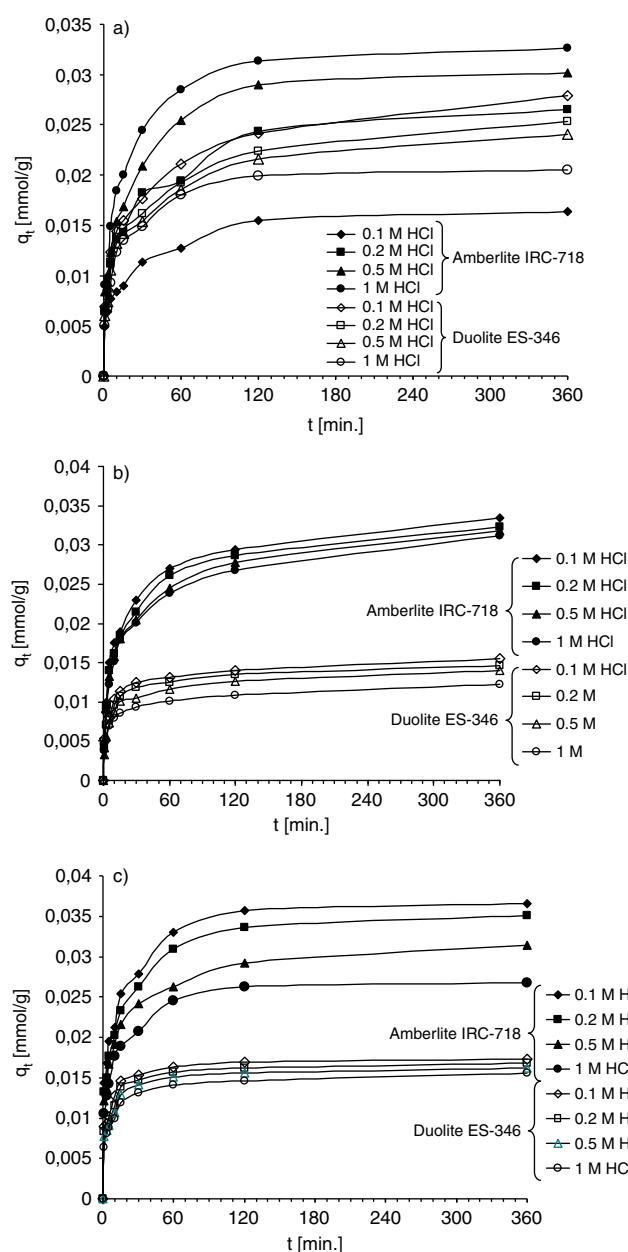


Fig. 4. Effect of macrocomponent addition on the amount of Pt(IV) adsorbed from the 0.1–1.0 M HCl – 1 M CuCl_2 – 0.55 mmol Pt(IV) I^{-1} (a), 0.1–1.0 M HCl – 1 M NiCl_2 – 0.55 mmol Pt(IV) I^{-1} (b) and 0.1–1.0 M HCl – 1 M AlCl_3 – 0.55 mmol Pt(IV) I^{-1} (c) systems using Amberlite IRC-718 and Duolite ES-346.

3.2.3. Kinetic parameters

In order to analyze the sorption of Pt(IV) on the chelating ion exchangers Amberlite IRC-718 and Duolite ES-346, the pseudo first order and pseudo second order kinetic models were applied to the experimental data. The comparison of the experimental results with the correlation coefficients in the 0.1 ÷ 3.0 M HCl – 0.55 mmol

Pt(IV) I^{-1} and 0.1–0.9 M HCl + 0.9–0.1 M HNO_3 – 0.55 mmol Pt(IV) I^{-1} systems is shown in Tables 3 and 4.

The values of k_1 and $q_{e,\text{cal}}$ for the pseudo first order kinetic model were obtained from the slopes and intercepts of the plots $\log(q_e - q_t)$ vs. t . The determination coefficients using the Lagergren model obtained at all studied initial concentrations were in the range of 0.7573–0.9036 and 0.6770–0.8982 for Duolite ES-346 and Amberlite IRC-718, respectively. However, the experimental $q_{e,\text{exp}}$ values did not agree with the calculated $q_{e,\text{cal}}$ data both in the chloride and chloride-nitrate media (Tables 3 and 4). This suggests that the adsorption of Pt(IV) on the chelating ion exchangers Amberlite IRC-718 and Duolite ES-346 did not follow the first-order kinetics.

Using Eq. (8), t/q_t was plotted against t ranging the initial dyes concentrations in order to calculate the second order rate constant k_2 and equilibrium adsorption capacity $q_{e,\text{cal}}$ from the slope and intercept, respectively. A good agreement between the experimental $q_{e,\text{exp}}$ and the calculated $q_{e,\text{cal}}$ values was obtained in the chloride and chloride-nitrate systems (Tables 3 and 4). It was found that the $q_{e,\text{cal}}$ values determined for Pt(IV) increased from 0.0173 to 0.0491 mmol g^{-1} and from 0.0295 to 0.0496 mmol g^{-1} with the decrease in the HCl concentration from 3 to 0.1 M using Duolite ES-346 and Amberlite IRC-718, respectively. In the mixed chloride-nitrate systems the $q_{e,\text{cal}}$ values increased with the decrease in HNO_3 concentration and agreed with the experimental values $q_{e,\text{exp}}$. The determination coefficients r^2 were very high, around 0.9999. This suggests that the studied sorption systems followed the pseudo second order kinetic model, based on the assumption that the rate limiting step may be chemical sorption or chemisorption involving valency forces through sharing or exchange of electrons between a sorbent and a sorbate. Mack et al. [25] confirmed the applicability of the pseudo-second order model for sorption of platinum(IV) chloro-species on yeast biomass.

The intraparticle diffusion model controls the sorption when the graph of q_t against $t^{0.5}$ is a straight line passing through the origin [18,26]. The values of r_i^2 were lower compared to those obtained from the pseudo second order kinetic model and indicated that Weber and Morris intraparticle diffusion model can not be applied for sorption of Pt(IV) on the chelating ion exchangers.

3.3. Column experiments

The weight (K_d) and bed (K_d') distribution coefficients as well as working (C_w) and total (C_t) ion exchange capacities were calculated from the breakthrough curves. The breakthrough curves for Pt(IV) depending on HCl and HCl/ HNO_3 concentrations using Amberlite IRC-718 are presented in Fig. 5.

Table 3
Kinetic parameters according to the pseudo-first order, pseudo-second order and intraparticle diffusion equations for Pr(IV) sorption on Duolite ES-346 from the chloride and chloride-nitrate systems

System	$q_{e,exp.}$	Pseudo-first order			Pseudo-second order			Fitting of pseudo-second order equation			Intraparticle diffusion	
		$q_{1,cal}$	k_1	r^2	$q_{2,cal}$	k_2	r^2	k_i	r_i^2			
0.1 M HCl	0.0488	52.2814	0.0279	0.7573	0.0491	7.2921	0.9999	18.5122	0.9142			
0.5 M HCl	0.0303	69.7627	0.0221	0.8004	0.0306	7.4578	0.9999	0.0019	0.4787			
1 M HCl	0.0218	110.1999	0.0299	0.7819	0.0219	15.6707	0.9999	0.0013	0.5709			
3 M HCl	0.0171	110.5926	0.0357	0.9036	0.0173	15.2139	0.9999	0.0008	0.5864			
0.1 M HCl + 0.9 M HNO ₃	0.0334	164.2345	0.0203	0.5576	0.0334	22.5537	0.9999	18.5122	0.9142			
0.5 M HCl + 0.5 M HNO ₃	0.0355	124.2848	0.0137	0.4425	0.0356	11.4427	0.9995	0.0009	0.2439			
0.9 M HCl + 0.1 M HNO ₃	0.0369	112.5669	0.0141	0.4865	0.0369	10.3378	0.9995	0.0009	0.2797			

$q_{e,exp.}$ [mmol g⁻¹]; $q_{1,cal}$ [mmol g⁻¹]; k_1 [1 min⁻¹]; $q_{2,cal}$ [mmol g⁻¹]; k_2 [g mmol⁻¹ min]; k_i [mmol g⁻¹ min^{0.5}].

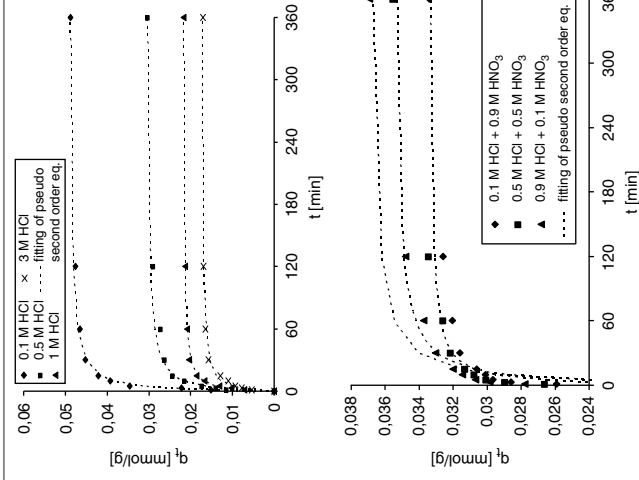
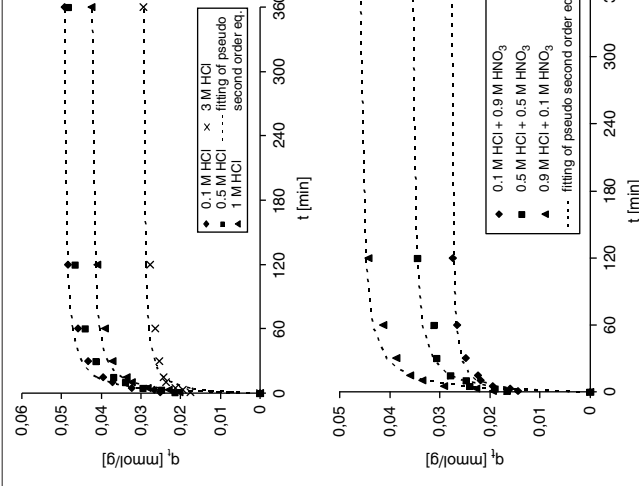


Table 4

Kinetic parameters according to the pseudo-first order, pseudo-second order and intraparticle diffusion equations for Pt(IV) sorption on Amberlite IRC-718 from the chloride and chloride-nitrate systems

System	$q_{e,exp}$	Pseudo-first order			Pseudo-second order			Fitting of pseudo-second order equation		Intraparticle diffusion	
		$q_{1,cal}$	k_1	r^2	$q_{2,cal}$	k_2	r^2	k_i	r_i^2		
0.1 M HCl	0.0492	46.2575	0.0289	0.8982	0.0496	6.3665	0.9999	16.7892	0.9057		
0.5 M HCl	0.0481	43.5934	0.0247	0.8780	0.0485	5.0441	0.9998	0.0018	0.5117		
1 M HCl	0.0424	56.0386	0.0237	0.8234	0.0427	6.8114	0.9998	0.0019	0.5676		
3 M HCl	0.0294	98.6453	0.0172	0.6770	0.0295	9.8362	0.9995	0.0009	0.4293		
0.1 M HCl + 0.9 M HNO ₃	0.0276	85.6736	0.0364	0.9283	0.0278	14.6434	0.9999	17.5842	0.9412		
0.5 M HCl + 0.5 M HNO ₃	0.0355	61.0770	0.0239	0.8629	0.0358	6.7729	0.9996	0.0010	0.4764		
0.9 M HCl + 0.1 M HNO ₃	0.0460	46.5438	0.0230	0.8496	0.0464	5.1439	0.9997	0.0014	0.5431		

$q_{e,exp}$ [mmol g⁻¹]; $q_{1,cal}$ [mmol g⁻¹]; k_1 [1 min⁻¹]; $q_{2,cal}$ [mmol g⁻¹]; k_2 [g mmol⁻¹ min]; k_i [mmol g⁻¹ min^{0.5}].



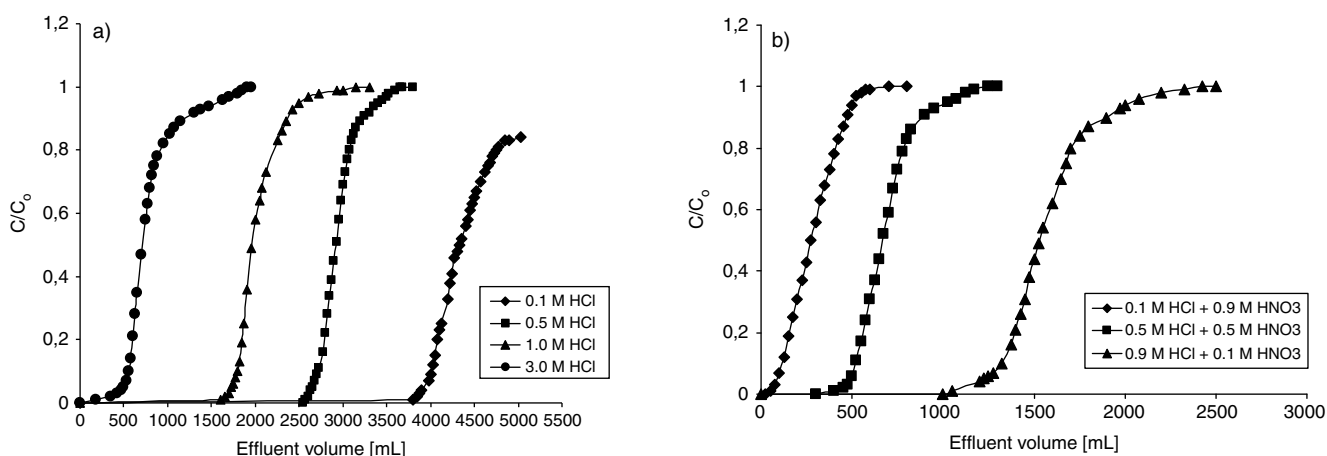


Fig. 5. Breakthrough curves of Pt(IV) from the 0.1–3 M HCl – 0.55 mmol Pt(IV) l⁻¹ (a) and 0.1–0.9 M HCl – 0.9–0.1 M HNO₃ – 0.55 mmol Pt(IV) l⁻¹ (b) systems using Amberlite IRC-718.

The working and total ion exchange capacities as well as the weight and bed distribution coefficients of Pt(IV) depend on hydrochloric acid concentration in the 0.1–3 M HCl system. The values under discussion decrease with the increasing hydrochloric acid concentration in the system for both chelating ion exchangers (Table 5). The same dependence was observed for the time required for the formation (t_f) and moving of the exchange zone (t_m).

In the 0.1–0.9 M HCl + 0.9–0.1 M HNO₃ systems the values of the ion exchange capacities of Duolite ES-346 and Amberlite IRC-718 determined from the breakthrough curves of Pt(IV) decrease with the increasing nitric acid content in the mixture of the total acids concentration 1 M. This fact can be explained by competitive sorption of nitrate ions or HCl₂⁻ ions towards [PtCl₆]²⁻ complexes. The times required for the formation and moving of the exchange zone in the mixed

Table 5

Weight (K_d) and bed (K'_d) distribution coefficients, working (C_w) and total (C_t) ion exchange capacities, time required for formation (t_f) and moving (t_m) of the exchange zone for Pt(IV) sorption from the chloride and chloride-nitrate solutions on Amberlite IRC-718 and Duolite ES-346

System	K'_d	K_d	C_w [mmol l ⁻¹]	C_t [mmol l ⁻¹]	t_f [min]	t_m [min]	Recovered [%]
Amberlite IRC-718							
0.1 M HCl	426.9	1704.9	209	235.1	4000.8	975.3	58.9
0.5 M HCl	286.4	1143.8	140.2	157.8	3025.5	995.2	67.6
1 M HCl	189.9	758.4	88	104.7	2627.4	1353.5	84.3
3 M HCl	65.6	261.9	9.6	36.4	1552.5	1413.2	42.3
0.1 M HCl + 0.9 M HNO ₃	26.9	107.4	1.3	15.1	636.9	617	17.9
0.5 M HCl + 0.5 M HNO ₃	66.4	265.2	16.5	71.5	1035	796.2	11.3
0.9 M HCl + 0.1 M HNO ₃	152.4	608.6	55	84.1	1990.4	1194.3	27.2
Duolite ES-346							
0.1 M HCl	331.4	596.0	121	182.6	5573.2	3821.7	65.6
0.5 M HCl	137.4	247.1	33	75.9	3960.9	3483.3	70.6
1 M HCl	60.4	108.6	11	33.5	3447.5	3288.2	77.6
3 M HCl	38.9	69.9	1.3	21.7	2149.7	2129.8	19.6
0.1 M HCl + 0.9 M HNO ₃	33.2	59.7	1.3	18.5	1401.3	1381.4	28.5
0.5 M HCl + 0.5 M HNO ₃	45.4	81.7	1.3	25.3	1791.4	1771.5	34
0.9 M HCl + 0.1 M HNO ₃	60.6	108.9	1.3	33.6	3542.9	3523.1	46.3

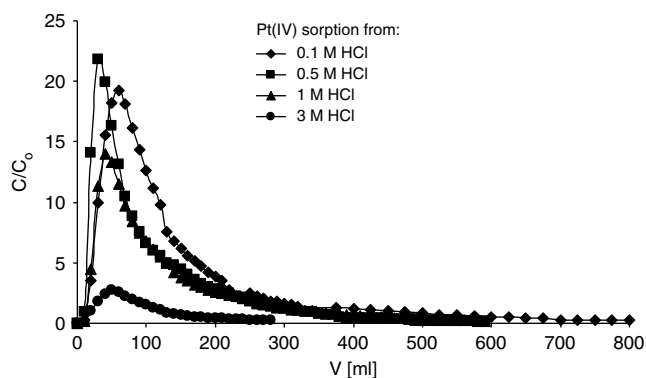


Fig. 6. Elution curves for Pt(IV) loaded on Amberlite IRC-718 using 6 M HCl as a desorbing agent for different sorption systems.

chloride-nitrate solutions are relatively shorter compared with the chloride systems.

Based on the total ion exchange capacities the applicability series of the chelating ion exchangers in the 0.1–3 M HCl – 0.55 mmol Pt(IV) l⁻¹ and 0.1–0.9 M HCl + 0.9–0.1 M HNO₃ – 0.55 mmol Pt(IV) l⁻¹ systems is as follows:

Amberlite IRC-718 > Duolite ES-346.

It is known that desorption of Pt(IV) from chelating ion exchangers is hardly achievable due to strong retention by functional groups of ion exchangers. That is why successful regeneration of the ion exchangers required the desorption agents which form more stable complexes with recovered ions than the complexes in the sorbent phase. In our studies we used 6 M hydrochloric acid and 1 M nitric acid for elution of Pt(IV) ions when the sorption of Pt(IV) was carried out from the 0.1–3 M HCl and 0.1–0.9 M HCl + 0.9–0.1 M HNO₃ systems, respectively. The desorption profiles for Amberlite IRC-718 are presented in Fig. 6. Table 5 summarized the amounts of Pt(IV) recovered in percentage. The best results (84.3% for IRC-718 and 77.6% for ES-346) were obtained using 6 M HCl as a desorbing agent while the sorption of Pt(IV) was in 1 M HCl. In the case of Pt(IV) sorption from the 0.1–0.9 M HCl + 0.9–0.1 M HNO₃ systems, the quantities of Pt(IV) desorbed by 1 M HNO₃ were equal to 27.2% and 46.3% for Amberlite IRC-718 and Duolite ES-346, respectively.

4. Conclusions

The chelating ion exchanger Amberlite IRC-718 of the iminodiacetate functional groups can be recommended for Pt(IV) ions removal from the anodic slimes, used up catalysts as well as Pt(IV) trace analysis because of their high affinity confirmed in the batch and column

studies. The Langmuir isotherm provided the best fit for the sorption of Pt(IV) on this ion exchanger. The kinetics followed the pseudo-second order equation. Desorption of Pt(IV) in the amount of 84.3% was obtained using 6 M HCl.

References

- [1] J. Minczewski, J. Chwastowska and R. Dybczyński, Separation and Preconcentration Methods in Inorganic Trace Analysis, John Wiley & Sons, New York, 1982.
- [2] O.N. Kononova, A.M. Melnikov, T.V. Borisova and A.S. Krylov, Simultaneous ion exchange recovery of platinum and rhodium from chloride solutions, Hydrometallurgy, 105 (2011) 341–349.
- [3] A. Wołowicz and Z. Hubicki, Comparison of strongly basic anion exchange resins applicability for the removal of palladium(II) ions from acidic solutions, Chem. Eng. J., 171 (2011) 206–215.
- [4] C.R.M. Rao and G.S. Redii, Platinum group metals (PGM): occurrence, use and recent trends in their determination, Trends Anal. Chem., 19 (2000) 565–586.
- [5] D. Jermakowicz-Bartkowiak, A preliminary evaluation of the use of the cyclam functionalized resin for the noble metals sorption, React. Funct. Polym., 67 (2007) 1505–1514.
- [6] K. Shams and F. Goodarzi, Improved and selective platinum recovery from spent α -alumina supported catalysts using pretreated anionic ion exchange resin, J. Hazard. Mater., B131 (2006) 229–237.
- [7] K. Shams, M.R. Beiggy and A. Gholamipour Shirazi, Platinum recovery from a spent industrial dehydrogenation catalyst using cyanide leaching followed by ion exchange, Appl. Catal. A, 258 (2004) 227–234.
- [8] K. Pyrzyńska, Recent advances in solid-phase extraction of platinum and palladium, Talanta, 47 (1998) 841–848.
- [9] J. Kramer, N.E. Dhladhla and K.R. Koch, Guanidinium functionalized silica-based anion exchangers significantly improve the selectivity of platinum group metal recovery from process solutions, Sep. Purif. Technol., 49 (2006) 181–185.
- [10] A. Ramesh, H. Hasegawa, W. Sugimoto, T. Maki and K. Ueda, Adsorption of gold(III), platinum(IV) and palladium(II) onto glycine modified crosslinked chitosan resin, Bioresour. Technol., 99 (2008) 3801–3809.
- [11] Z. Hubicki, M. Leszczyńska, B. Łodyga and A. Łodyga, Palladium(II) removal from chloride and chloride–nitrate solutions by chelating ion-exchangers containing N-donor atoms, Miner. Eng., 19 (2006) 1341–1347.
- [12] Z. Hubicki, A. Wołowicz and M. Wawrzekiewicz, Application of commercially available anion exchange resins for preconcentration of palladium(II) complexes from chloride-nitrate solutions, Chem. Eng. J., 150 (2009) 96–103.
- [13] I. Kiran, T. Akar, A.S. Ozcan, A. Ozcan and S. Tunali, Biosorption kinetics and isotherm studied of acid red 57 by dried *Cephalosporium aphidicola* cells from aqueous solutions, Biochem. Eng. J., 31 (2006) 197–203.
- [14] A. Wołowicz and Z. Hubicki, Effect of matrix and structure types of ion exchangers on palladium(II) sorption from acidic medium, Chem. Eng. J., 160 (2010) 660–670.
- [15] V. Vadivelan and K.V. Kumar, Equilibrium, kinetics, mechanism and process design for the sorption of methylene blue onto rice husk, J. Colloid. Interface Sci., 286 (2005) 90–100.
- [16] K.V. Kumar and S. Sivanesan, Selection of optimum sorption kinetics: comparison of linear and non-linear method, J. Hazard. Mater., 134B (2006) 277–279.
- [17] C.L. Mack, B. Wilhelm, J.R. Duncan and J.E. Burgess, A kinetic study of the recovery of platinum ions from an artificial aqueous solution by immobilized *Saccharomyces cerevisiae* biomass, Miner. Eng., 21 (2008) 31–37.
- [18] Y.S. Ho and G. McKay, Sorption of dyes from aqueous solution by peat, Chem. Eng. J., 70 (1998) 115–124.

- [19] C.E. Harland, *Ion Exchange: Theory and Practice*, Royal Society of Chemistry Paperbacks, Cambridge, 1994.
- [20] F.L. Bernardis, R.A. Grant and D.C. Sherrington, A review of methods of separation of the platinum-group metals through their chloro-complexes, *React. Funct. Polym.*, 65 (2005) 205–217.
- [21] I.A.W. Tan, A.L. Ahmad and B.H. Hameed, Adsorption of basic dye on high-surface-area activated carbon prepared from coconut husk: equilibrium, kinetic and thermodynamic studies, *J. Hazard. Mater.*, 154 (2008) 337–346.
- [22] H. Lata, V.K. Garg and R.K. Gupta, Adsorptive removal of basic dye by chemically activated parthenium biomass: equilibrium and kinetic modeling, *Desalination*, 219 (2008) 250–261.
- [23] K. Ada, A. Ergene, S. Tan and E. Yalçın, Adsorption of remazol brilliant blue R using ZnO fine powder: equilibrium, kinetic and thermodynamic modeling studies, *J. Hazard. Mater.*, 165 (2009) 637–644.
- [24] V.I. Inglezakis, Solubility-normalized Dubinin–Astakhov adsorption isotherm for ion-exchange systems, *Micro. Meso. Mater.*, 103 (2007) 72–81.
- [25] C.L. Mack, B. Wilhelmi, J.R. Duncan and Jh.E. Burgess, A kinetic study of the recovery of platinum ions from an artificial aqueous solution by immobilized *Saccharomyces cerevisiae* biomass, *Miner. Eng.*, 21 (2008) 31–37.
- [26] Y.S. Ho, Second-order kinetic model for the sorption of cadmium onto tree fern: a comparison of linear and non-linear methods, *Water Res.*, 40 (2006) 119–125.